Thin-Walled Structures, Volume 54, May 2012, Pages 44–53

Non-Linear Idealisation Error Analysis of a Metallic Stiffened Panel Loaded in Compression

Authors: J. Campbell, L. Hetey and R. Vignjevic
Crashworthiness, Impact & Structural Mechanics Group,
School of Engineering, Cranfield University, Cranfield, MK43 0AL, UK

Abstract

The SAFESA procedure is an idealisation error control process developed for linear static finite element (FE) analysis. This paper investigates the application of this process to non-linear FE in order to provide an equivalent methodology valid for non-linear problems. The post-bucked collapse of a stiffened panel in compression is used as the case study for this investigation. The main part of the paper presents the critical analysis of important modelling assumptions, including the material model, the panel to stiffener contact, boundary conditions and geometrical imperfections. Several potential idealisation error sources are identified using the process and then investigated using the non-linear FE code ABAQUS. The outcome of the analysis is an improved FE model and a quantification of the idealisation error, showing that the idealisation error control process can be applied to non-linear analysis

Keywords: FEM, Modelling, Error control, Idealisation, Abaqus, Non-linear

1. Introduction

Stiffened Panels are basic components for the construction of airplanes and ships. For a safe design it is crucial to understand the behaviour of these structures under compression and to predict the ultimate strength [1-3]. This is especially important for virtual testing in the certification process of new products.

The focus of this paper is to study the FEM idealisation process for non-linear analyses, and to analyse potential error sources. This is done by applying an idealisation error control process, based on the SAFESA procedure [4,5] which was previously developed at Cranfield University for linear static analyses. The aim is to improve the reliability of simulation results, and demonstrate that the SAFESA method can be applied to non-linear problems [6]. All analyses were performed using Abaqus/Standard [7].

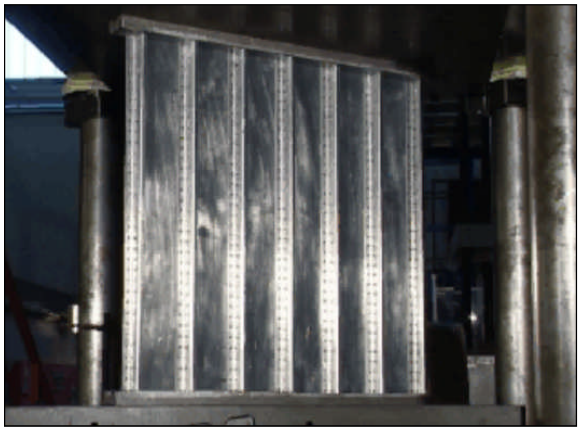

Figure 1: Stiffened Panel Test

To demonstrate the idealisation error control process, an example of a stiffened panel in compression is used. The panel consists of seven aluminium Z-section stiffeners riveted to the aluminium skin, Fig. 1. The panel design is used at Cranfield for a class exercise in the post-buckled design of stiffened panels. In several tests an ultimate failure load between 97 and 103 kN was measured. The test machine available does not allow the recording of the load vs. displacement curve to be recorded. Therefore the experimental results are not suitable for use as a validation of the FE analysis.

This paper is organised as follows: Section 2 introduces the idealisation error control procedure. Section 3 presents results of stiffened panel design calculations and section 4 describes a first FEM model. In section 5 is the analysis of potential error sources described. Final outcome is an improved FE model and estimation of the involved error.

2. Idealisation Error Control Procedure

SAFESA (SAFE Structural Analysis) is a procedure for formally controlling idealisation errors in linear static analysis [4,5]. The aim of the method is to provide a systematic procedure whereby an engineer is able to perform an analysis of a structure in such a way that errors which may occur as a result of the idealisation process are controlled.

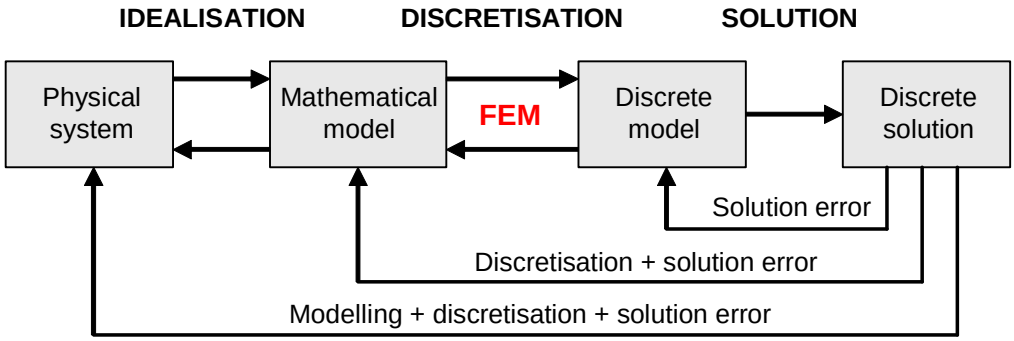

Figure 2: The FE Analysis Process

The idealisation process represents the step of converting the real-world structure into an idealised mathematical model of the structure that can be practically modelled using the finite element method (FEM), Fig. 2. Within this process the analyst is required to make a series of assumptions, generally simplifications, which contribute to the error in the final analysis. Analysis input is a description of the real world problem (drawings, CAD model …) and the output is a description of the structure ready for meshing. Information is fed from one step to the next in a linear sequential manner and includes possible feedback loops, i.e. the process can be iterative. A flagging technique is used to determine that errors at a specific step in the method have not been adequately treated and must be analysed at a later stage. The procedure consists of the following steps:

- **Step 1 & 2: Global idealisation, such as boundaries, boundary conditions, loading, load paths and geometry idealisation for the structure as a whole.** Geometrical simplifications such as omitting unnecessary structural details such as bolt holes or curved corners can be made. Boundary conditions and loading actions have to be chosen in a way that they conform with the FEM modelling capabilities. Error bounds are estimated and all ambiguity is flagged out for later investigation.
- **Step 3: Decomposition of the structure into features and primitives.** A feature represents a recognisable entity which exhibits coherent structural properties. The main idea behind this step is the study of feature interconnections, and the decomposition of a big problem into smaller ones.
- **Step 4 & 5: Repeating the first two steps at the feature and primitive level.** New boundary conditions and loading actions have to be derived from feature contact surfaces. This process may follow directly from the definitions at a higher level, but in general will require more detailed description here.
- **Step 6: Assessment of the performed analyses so far.** Either error bounds can be directly assessed or additional testing (**Step 7**) will be necessary. This step also requires the planning of all sensitivity studies, hierarchical modelling and test programmes to address uncertainties which have been identified in steps 1 to 5.
- **Step 7: Run the test program.** Execution of corroborative tests. The results will be compared with the assumed behaviour. If the assumptions were inappropriate, they get adapted to the test result.

During the idealisation process, the following error sources can be identified:

- **Mathematical model** – The derivation of a mathematical model employs physical laws, mathematical manipulation and approximations. Each approximation introduces simplifications and associated errors.
- **Domain** – Very often errors are generated by eliminating geometric details. In most cases, domain simplifications are carried out on the basis of previous experience in the solution of similar problems.
- **Material properties** – Material parameters are probabilistic in nature and have to be specified. Any deviation from the correct values introduces error into the solution.

- **Boundary conditions, loading** – These input parameter are often difficult to abstract from the physical situation as reasonable simplifications need to be made. Very often structures are modelled with a built-in support by removing all degrees of freedom at the involved nodes. This simplification does not exist in reality.

Experience rules, simple calculations, experimental tests, hierarchical modelling and sensitivity analyses are the tools for analysing the errors. By gaining experience, analysts develop and document specific sets of idealisation rules that are appropriate to their specific class of problems. Hierarchical modelling means changing the level of idealisation. The whole structure is decomposed into features and primitives, and the resultant smaller problems will be solved. Sensitivity analyses study the effect of small changes in the value of input parameters on the resultant output parameters. Input parameters comprise material properties, domain and boundary conditions.

3. Stiffened Panel Design Calculations

The classical approach to predicting the ultimate load of a stiffened panel in the aircraft industry is design calculations using simplified theory and data sheets such as those published by ESDU [8]. The outcome of this calculation will help to understand the structural behaviour and is an important step towards a realistic model. When loading stiffened panels axially different failure modes occur and the design calculations allow an applied load to be determined for each mode, Table 1:

Failure Mode	Applied Load [kN]
Skin local buckling between stiffeners	20
Torsional buckling of outer skin-stiffener	101
Flexural (Euler) buckling of skin-stiffener	110
Inter-rivet buckling	143
Stringer crippling	144

Table 1: Design calculation results for the panel

Skin local buckling is not a global failure mode. All other failure modes lead to collapse of the structure, with torsional buckling at 101 kN as the critical failure mode.

These calculations assume a perfect geometry and a uniformly applied load. It should be noted that this panel design places stringers along the free edges. In real aerospace structures the boundary condition along the sides would provide a stiffer constraint, and the failure mode would then be flexural buckling.

4. Initial FEM Model

The panel consists of a rectangular plate (length: 500 mm x width: 492 mm x thickness: 0.9 mm). The plate is stiffened by seven Z-shaped stiffeners (length: 500 mm x thickness: 0.9 mm; height: 20 mm, top-section: 8 mm, bottom-section: 12 mm), Fig. 3. Stiffeners are riveted on the plate with a rivet pitch of 14 mm. The rivets (snap

head SP80) have a diameter of 2.38 mm. Plate and stiffener are made of aluminium L165 (2014A-T6), the rivets of aluminium L69.

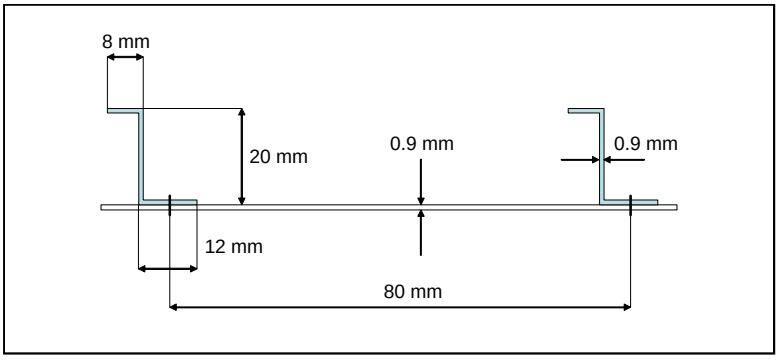

Figure 3: Side View of the Panel Idealisation

The three-dimensional panel assembly is modelled with shell elements. Both ends of the panel are cast into a prismatic Cerrobend (an alloy of bismuth, lead, tin and cadmium) fitting. The panel is placed in the test machine without additional fastening, Fig 1. The upper plate of the test rig is fixed and the lower plate moves upwards in order to compress the panel. In the FEM model these are idealised as the boundary conditions shown in Fig. 4. Side C is clamped, as all degrees of freedom are fixed. Side A is moving axially in direction towards side C. This is realised with multipoint constraints (MPC). Sides B and D are not constrained, as in the real test.

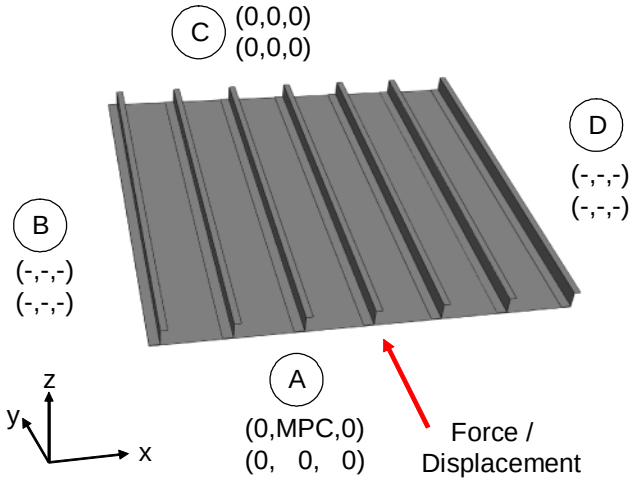

Figure 4: FEM geometry with boundary conditions

A mesh sensitivity study investigating different shell element types (S4R5, S4R, S4, S8R5, S8R) and number of elements (2464, 10584, 42336) showed that 10584 S4R elements were sufficient for this first model [6]. The geometrically non-linear analysis uses a modified Newton-Raphson method (in Abaqus using the syntax *step, nlgeom) with stabilisation (in Abaqus: *static, stabilize) and default parameters [7]. A further sensitivity study showed that the Abaqus default stabilising factor works well. Lower values lead to convergence problems and higher values increased the panel failure load artificially. The panel-stiffener connection is represented using merged

nodes at the contact interface, Fig. 7 - node_equ_edge. Panel failure is defined as a drop in the load-shortening curve.

5. Idealisation Error Analysis using SAFESA

Application of SAFESA flagged out the following error sources [6]:

- material model
- applying load or displacement
- contact between panel and stiffener
- sensitivity to boundary conditions
- shape of the stiffeners
- geometrical imperfections
- scattering in material parameters
- accordance with predicted failure modes

The model was improved iteratively, and a comparison between solutions is made on the basis of the results within each error source. The resulting error is the relative change in failure load of the reference model when applying an alternative idealisation. The obtained error values were finally rounded to percent values.

5.1 Material Model

Material parameters obtained directly from coupon tests would increase the model reliability but were not carried out within this project, see section 5.7. The panel design [6] states that the material used conforms to aluminium L165 (2014A-T6) with:

Modulus of elasticity E = 68000 N/mm^2
Poisson's ratio v = 0.33
Yield stress σ_y = 340 N/mm^2

In buckling analyses it is common to model the non-linear behaviour of metals using the Ramberg-Osgood model [9], and this was used as a basis for the material properties in the FE model. The stress-strain relation was calculated using tabulated material data [10] and Equ. 1:

$$\varepsilon = \frac{\sigma}{E} + \frac{f_n}{Em}\left[\frac{\sigma}{f_n}\right]^m \qquad (1)$$

For L165 the material parameters are [10]: f_n = 296 N/mm^2 and m = 17.

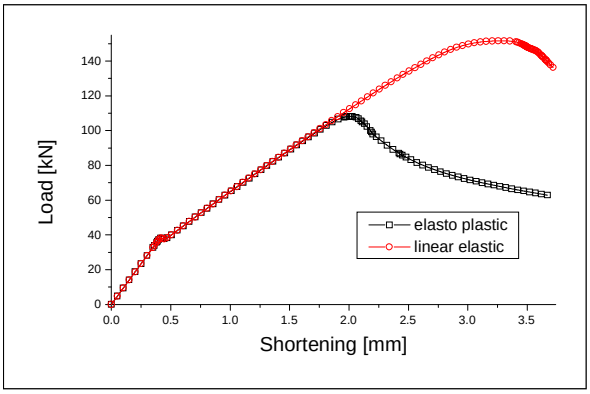

Figure 5: Linear vs. Non-linear Material Model

Using non-linear material properties is crucial as can be seen in Fig. 5. However the Ramberg-Osgood model is still an approximation to the true material behaviour and its use is source of idealisation error, see Collette [11] and references therein. The Ramberg-Osgood model is a good approximation to the behaviour of aluminium in compression and a maximum idealisation error of 1% is assumed from its use. The uncertainty from the material properties used is a separate error source and is dealt with in section 5.7.

5.2 Applying Load versus Displacement

The hydraulic test rig used is actually load controlled. This means load is applied and the resulting displacement is measured. The problem with a load controlled FE analysis is that the applied load is always increasing and the moment of panel failure cannot be accurately determined.

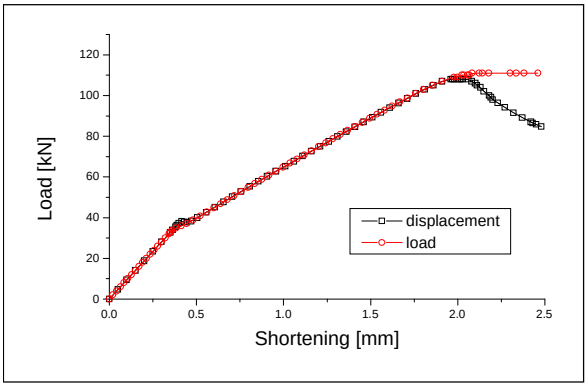

Figure 6: Displacement vs. Load Controlled Analysis

Fig. 6 compares the effect of doing a load or a displacement controlled analysis. The models predict a very similar load-shortening graph up to panel failure. At the critical displacement the sustained load differs by less than 0.2%. Therefore, the displacement controlled analyses will be used further without including a modelling error.

5.3 Contact between Panel and Stiffener

The panel-stiffener contact, Fig. 3, can be modelled in different ways. An appropriate contact modelling for the stiffener and panel surfaces, and a model for the rivets have to be found. The actual shape of the rivets and the rivet holes in the plates are neglected, as there are too many (7x36=252) and the mesh resolution required to specifically represent the hole and rivet geometry is impractical. In ten compression tests of the panel design, none of the rivets failed. The assumption to neglect the rivet failure modelling is therefore justified. However, the ductile behaviour of the rivets must be taken into account.

5.3.1 Simple Contact Models

The simplest model node_equ_edge uses a rigid shell connection. The stiffener top is directly connected to the plate elements, using the same nodes, Fig. 7. The strength of this structure will be lower than what occurs in reality, because the stiffener bottom is neglected.

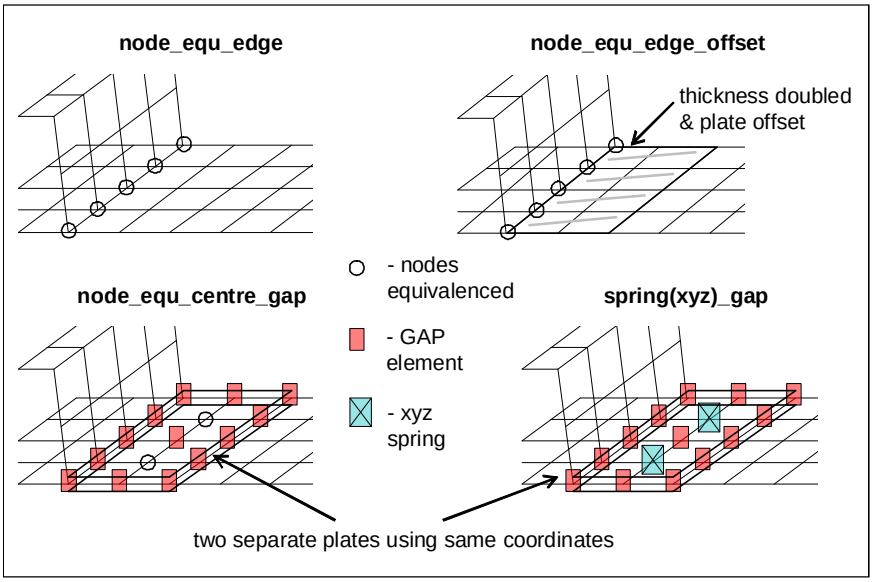

Figure 7: Simple Contact Models

Table 2 lists the results using the first model node_equ_edge, and modifications of it. In node_equ_edge_offset the plate thickness along the contact area was doubled and given a shell offset upwards. This idealisation leads to a solution that is too stiff as two plates in contact have less residual strength then a single plate with the combined thickness.

Model	Collapse Load [kN]
node_equ_edge	108.12
node_equ_edge_offset	140.41
node_equ_centre_gap	121.20
spring(xyz)_gap	118.86

Table 2: Simple Contact Models

The other simulations model the base of the z-stringer explicitly, where the rivets are represented using a combination of GAP elements, springs and equivalencing nodes at the corresponding locations, Fig. 7. In nod_equ_centre_gap and spring(xyz)_gap, every second node along the midline of the stiffener-plate interface was equivalenced or connected with xyz-springs. The remaining opposing nodes were connected via GAP elements. The springs were oriented in x-, y- and z-directions. The stiffness was determined to represent the material used for the rivets. The collapse load of these models lies between that of the previous two. The model spring(xyz)_gap is the most realistic, but need to be investigated further.

5.3.2 Rivet and Contact Modelling

Rivets connect the stiffeners to the panel. As the rivets slightly deform but do not fail, different modelling approaches need to be considered. Abaqus [7] offers the following joint models:

Multi-point constraints (MPC's) allow constraints to be imposed between different nodes of the model. This is an efficient approach, as it reduces the size of the problem. Out of the Abaqus library of MPC's, the following constraints are of interest here:

- **mpc_beam** constrains the displacement and rotation at the first node to the displacement and rotation at the second node.
- **mpc_link** keeps the distance between the two nodes constant.
- **mpc_pin** makes the displacements of the two nodes equal.
- **mpc_tie** makes all active degrees of freedom at the two nodes equal.

In contrast to MPC's, connector elements do not eliminate degrees of freedom, instead the constraints are enforced with Lagrange multipliers. The following connectors will be tested:

- **conn_beam** has the functionality as mpc_beam.
- **conn_link** has the functionality as mpc_link.
- **conn_weld** has the functionality of conn_beam (mpc_beam); in addition the node locations will be joined.
- **conn_cartesian** provides a connection between two nodes that allow independent behaviour in three local Cartesian directions. This behaviour can be elasticity, plasticity, damage, failure or friction. The elasto-plastic parameters used in this analysis were calculated from rivet dimension, measured plastic deformation and published material properties [10].

Using **beams** can be considered the most realistic approach, as rivets behave like small beams. The problem with this approach is that the resulting beam elements are very short, and can generate numerical instabilities.

Contact between the stiffeners and skin can be modelled using contact elements (GAP's) or with a surface based approach. Furthermore, one needs to decide if the mesh of the two surfaces in contact lie on the same plane or are offset to represent the material thicknesses. There are four contact variations as shown in Fig. 8:

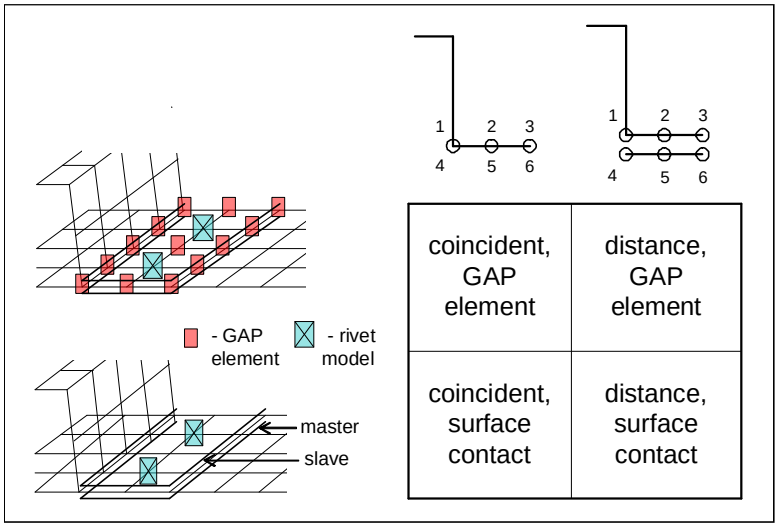

Figure 8: Different Contact Variations

Gap elements define contact between nodes. It allows nodes to be in contact (gap closed) or separated (gap open) with respect to particular directions.

Surface contact is more practical [7], as gap elements do not need to be created. Instead the two surfaces where the contact algorithm will be applied need to be defined.

Abaqus offers diverse contact formulations: finite-sliding versus small-sliding, and node-to-surface versus surface-to-surface. All analyses in this investigation use the surface-to-surface together with finite-sliding contact formulation, as it demonstrated to be the most stable.

Table 3 compares failure loads of all possibilities to model contact and the rivets. For the coincident-node geometries fewer rivet models are available; beams, conn_beam, mpc_beam and mpc_link need a real length for their definition.

	Coincident		**Distance**	
	Model	Collapse Load [kN]	Model	Collapse Load [kN]
GAPUNI Contact Element	conn_beam_gap	119.20	conn_beam_gap	122.55
	conn_cart_gap	118.86	conn_cart_gap	120.54
			conn_link_gap	114.44
	conn_weld_gap	119.20	conn_weld_gap	122.55
			mpc_beam_gap	122.55
			mpc_link_gap	114.43
	mpc_pin_gap	119.31	mpc_pin_gap	118.45
	mpc_tie_gap	119.20	mpc_tie_gap	119.20
			beam_gap	(124.87)*

*not converged

	conn_beam	119.88	conn_beam	122.22
	conn_cart	117.85	conn_cart	119.67
Surface			conn_link	114.93
Based	conn_weld	119.88	conn_weld	122.22
Contact			mpc_beam	122.22
			mpc_link	115.13
	mpc_pin	118.22	mpc_pin	117.16
	mpc_tie	119.97	mpc_tie	120.08
			beam	(120.09)*

Table 3: Distance Surface Models

All models converged, except for the beam models. This is due to stability problems from using such short beams to connect two contact surfaces. The collapse load varies between 114.43 and 122.55 kN, a difference of around 7%.

The correct joint model is bounded between two extremes. conn_beam and mpc_beam model a rigid connection, which is too stiff. conn_link and mpc_link on the other hand model a joint that is too loose. The conn_cart connector is able to model best the rivet deformation. This element allows the definition of the specific stiffness and can be extended for more complicated rivet models, e.g. failure.

Gap element and surface based contact showed very similar solution behaviour. The difference between coincident and distance models is that conn_beam, conn_cart and conn_weld behaved stiffer in the distance models. The most realistic contact idealisation involves using a distance, which is more in line with the physical setup. The surface based contact seems to cope better with complex geometry non-linearity then contact using gap elements.

The surface based contact with distance and Cartesian connector elements that were finally selected make the FE model more realistic compared to the first model node_equ_edge. The collapse load increased from 108.12 to 119.67 kN. An idealisation uncertainty of 1% will remain due to the chosen distance contact model (“conn_cart_gap” vs. “conn_cart”). A small uncertainty will also remain as the rivet properties were calculated using engineering assumptions.

5.4 Sensitivity to Boundary Conditions

This error investigation is motivated by the fact that the panel is not rigidly connected to the test machine and minor rotation around the end axes can occur. The top and bottom ends of the panel are cast into Cerrobend and the ends of the panel remain in direct contact with the test rig, Fig. 1. The Cerrobend adds additional stiffness to both ends and prevents movement and rotation of the panel during the test.

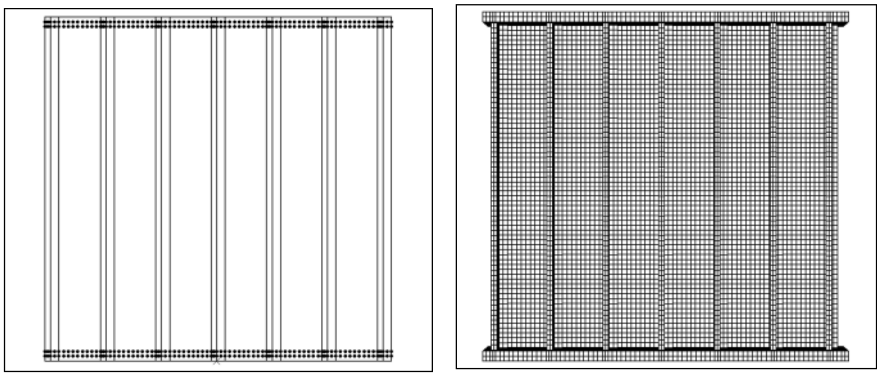

Figure 9: “constraint band” and “Cerrobend modelled”

Fig. 9 illustrates boundary condition idealisations. The figure highlights the nodes of the constraint band. Model “Ends cast + constraint band cast” constrains all involved nodes using MPC’s. This shortens the panel by the length of the Cerroband. “End cast + constraint band” casts the ends nodes and allows only an axial displacement of the nodes in the constraint band. “Cerrobend modelled” models the Cerrobend explicitly with solid elements. The elastic stiffness was estimated to be 10% of the aluminium used. The solid elements were connected to the panel shells using a tied surface (in Abaqus syntax *tie). MPC constraints were used to represent the test machine.

Model	Collapse Load [kN]
Ends cast (reference)	119.71
Ends cast + constraint band cast	118.30
Ends cast + constraint band	116.60
Cerrobend modelled	114.65
Free rotation around ends	71.92

Table 4: Boundary Conditions

The true model will lie between “Ends cast (reference)” and “Free rotation around ends”, see Table 4. “Free rotation around ends” means in FEM language constraint (0,0,0,0,0,0) versus (0,0,0,-,0,0). Allowing the panel to rotate around the axes of the ends has a big impact on the collapse load, but is a too big exaggeration of the actual panel end flexibility.

Including the Cerrobend in the model seems sensible, but the brittle material behaviour was not modelled. “Ends cast + constraint band” seems to be more realistic and will be used in an improved model. The effect of including the constraint band is that the local buckling shape changes from 4 to 3.5 wavelengths (see section 5.8) along the panel lengths. As the end platen flexibility is not perfectly modelled an idealisation error of 3% (“Ends cast (reference)” vs. “Ends cast + constraint band”) will be left.

5.5 Shape of the Stiffeners

In the initial model, Fig 4., the stiffeners were modelled with square corners, which is a simplification of the structure. Fig. 10 illustrates the real shape of a stiffener, showing the curved corners.

Figure 10: Curved Shape of a Stiffener

Modelling a curved shape with the FEM adds complexity, as the mesh size has to be smaller to correctly capture the geometry.

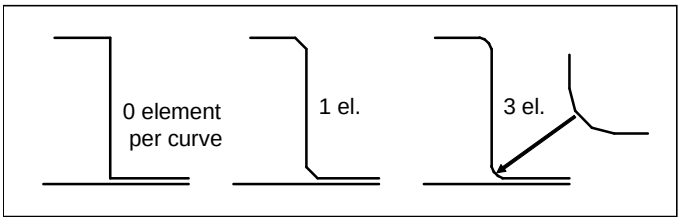

Figure 11: Idealisation of curved Panel Corners

Fig. 11 shows different idealisations of the curved stiffener shape. “0 element per curve” is the reference model. “1 el.” uses one, and ”3 el.” uses three additional shell elements for one curve. A drop in ultimate strength for the more curved models is the result, see Table 5.

Model	Collapse Load [kN]
Reference	119.37
1 element per curve	117.86
3 elements per curve	118.79

Table 5: Impact of Edge Curvature

The authors believe that the decrease in collapse load is caused by shortening the contact area. The stiffener contacts an area of length times 12 mm in the reference model, Fig. 3. In the one and three “element per curve” models it shortens to length times 10 mm. Due to distortions the real contact area can even become smaller, Fig. 10. The stiffener-plate contact area is the most stabilising part of the whole panel, as it has the biggest thickness. Disturbances in this area affect the whole panel. An improved model must take this into account. An idealisation error of 1% (“Reference” vs.”1 element per curve”) will remain.

5.6 Geometrical Imperfections

A Cyclone Series 2 digitising system from Renishaw was used to scan the panel surface. This machine has a resolution of 5 µm. The surface was scanned with a

distance of 2 mm between each point in x- and y-direction. The coordinates and associated z-values were recorded. The analysis of the scan data revealed that the panel differs systematically from a flat surface, with the panel becoming slightly curved following the Cerrobend casting.

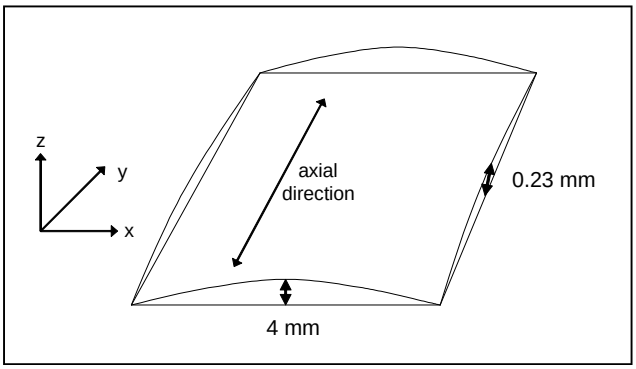

Figure 12: Systematic Geometrical Imperfection

Fig. 12 illustrates that the panel is arched 4 mm along its top and bottom sides and 0.23 mm axially. This curved shape is the new “perfect” geometry. To obtain magnitudes of local imperfections, the difference of the scanned surface and the curved shape was analysed.

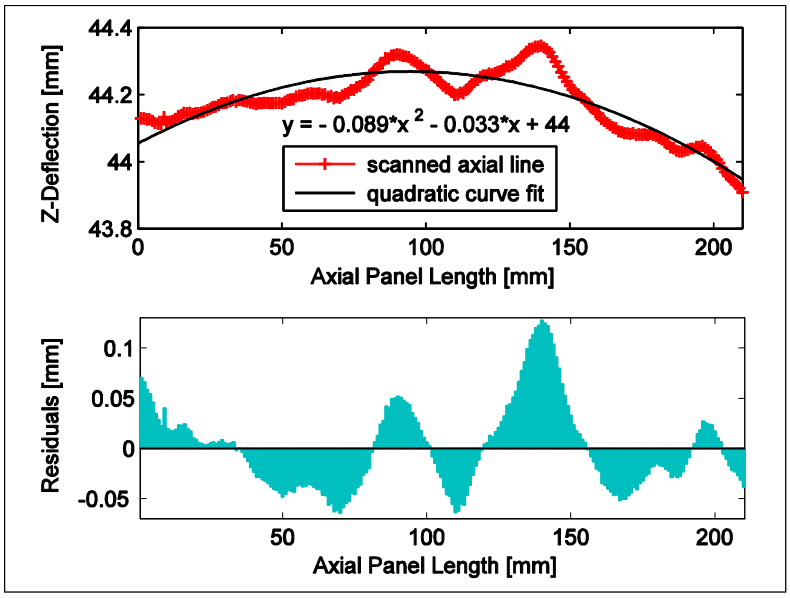

Figure 13: Quadratic Curve Fit and Residuals along Panel Axis

Fig. 13 shows the analysis of one representative “scanned axial line” using MATLAB. A “quadratic curve fit” using the Eulerian least square method was calculated, which maps the axial curvature of 0.23 mm. The difference between both lines is plotted as residuals in the bottom graph. These residuals determine the imperfection per scan line. Because the imperfection per scan line will be smoothed through the quadratic fit within each line, the global imperfection was calculated as well. This is done by averaging all scanned lines and calculating a curve fit of this average. The residuals of the global curve fit and each scanned line determine the global imperfection.

Imperfections	Average [mm]	Maximum [mm]
Per axial scan line	0.02	0.18
Global	0.05	0.57

Table 6: Local and Global Imperfection

Table 6 shows the imperfection magnitudes. The maximum imperfection per scan line is 0.18 mm and the maximum global imperfection 0.57 mm. This corresponds to about 20% and 60% of the panel thickness respectively.

There are three possibilities to add imperfection to a FEM model:

1. generating a new mesh, which includes the imperfection,
2. adding the shape of a buckling mode,
3. changing directly coordinates of nodes.

The first option is the most elaborate because an entirely new model has to be created. The other two options can be performed easily with the ABAQUS command *Imperfection.

5.6.1 Systematic Imperfection

A new mesh was generated to map the panel shape of Fig. 12. The collapse load decreased only slightly, see Table 7. It appears that there is a trade-off for the two curvatures. The axial bending weakens the structure, but the side bending stiffens the structure. The panel was slightly transformed into a stiffer cylindrical structure.

Model	Collapse Load [kN]	Solution Increments
Reference	119.34	161
Systematic Imperfection	118.99	482

Table 7: Impact of Systematic Imperfection

Using the curved shape introduced numerical difficulties. The analysis converged only after experimenting with different solver parameters. The convergence problems were caused by using initially curved surfaces together with the selected contact algorithm.

5.6.2 Eigenmode Imperfection

A standard procedure to incorporate geometrical imperfections is to add the shape of an eigenmode [1-3]. The first eigenmode represents the theoretical initial buckling shape, i.e. the shape the panel will most likely deform into. Table 8 shows the impact of adding different magnitudes of the first eigenmode. Depending on the magnitude, the collapse load decreases. Also, the effect of applying different eigenmodes was studied. The first, second and third eigenmode were added with a magnitude of 100% panel thickness. The collapse load decreased most for the first eigenmode and least for the third mode.

Model	Collapse Load [kN]
Reference	119.34
1st eigenmode, 1% panel thickness	118.89
1st eigenmode, 10% panel thickness	117.27
1st eigenmode, 100% panel thickness	114.93
2nd eigenmode, 100% panel thickness	115.05
3rd eigenmode, 100% panel thickness	118.73

Table 8: Impact of Eigenmodes

Applying eigenmode imperfections decreases the panel stiffness for certain modes. But the analysis of the scan data did not show that the imperfections have an eigenmode shape.

5.6.3 Local Imperfection

Table 9 displays the impact of applying local imperfections. These imperfections were added to the mesh with the magnitude of the measured values (about 50% panel thickness), and also approximately with their geometrical distribution.

Model	Collapse Load [kN]
Reference	119.34
Local Imperfection 5% panel thickness	120.13
Local Imperfection 50% panel thickness	119.36
Local Imperfection 500% panel thickness	118.79

Table 9: Different Magnitudes of Local Imperfections

These results indicate that the panel collapse behaviour is insensitive to small local imperfections. Therefore, it depends where the imperfection is applied. Even big dents added to the plate between two stiffeners do not significantly affect the panel failure behaviour. Imperfections around critical areas, such as the middle of the outer stiffeners where the panel collapse process begins, have a much larger influence. A local imperfection of 50 % panel thickness will be included into the improved model as this approximates the actual variation measured in the scans.

5.7 Scattering in Material Parameters

This error source is strongly linked to the material model. Material properties can vary greatly and depend on temperature, thickness, production process and the alloy composition. Alloy specifications are not too definite [12], e.g. the proportion of copper in aluminium L165 may vary by 1.1% (3.9-5.0%). In order to obtain reliable information, specimen tests with the panel material would be necessary. It was not possible to assemble statistically significant data within the scope of this research. Therefore, published data were consulted. ESDU [12] and MIL-HDBK-5H [13] both specify mean values for elasticity and yield stress for the used alloy, but do not specify variability. Haugen [14] lists specific values of alloys similar to the used L165 (2014A-T6), see Table 10.

Material	Tensile Yield Strength			
	Mean [N/mm^2]	Mean [ksi]	Standard Deviation	Sample Size
2014 (AMS 4135)	(517.13)	63.0	1.75	20
2014-T651	(496.44)	72.0	2.07	19
2024-T4	(248.91)	36.1	1.91	61

Table 10: Variation in Static Strength of Aluminium Alloys [14]

Published yield strength was given in ksi units and was transformed in the table to $\mathrm{N/mm^2}$ using the factor 6.895 [13]. Simulated test data were generated using random normal distributions with a mean value of 0.0 and a standard deviation of 1.0. These distributions were transformed to the parameters of the elasto-plastic material model (using the Abaqus *Parameter command). With n=100 repetitions and a reference value of 119.30 kN, the failure loads were in the interval [118.21 .. 120.62] kN. The final model will use the producer supplied mean values. An idealisation error of 1% (119.30 kN vs. 120.62 kN) results when simulating the test data.

5.8 Accordance with Predicted Failure Modes

From the design calculations, section 3, local skin buckling should start at 20 kN; and torsional buckling of the outer skin-stiffener at 101 kN was predicted as the collapse mode of the panel.

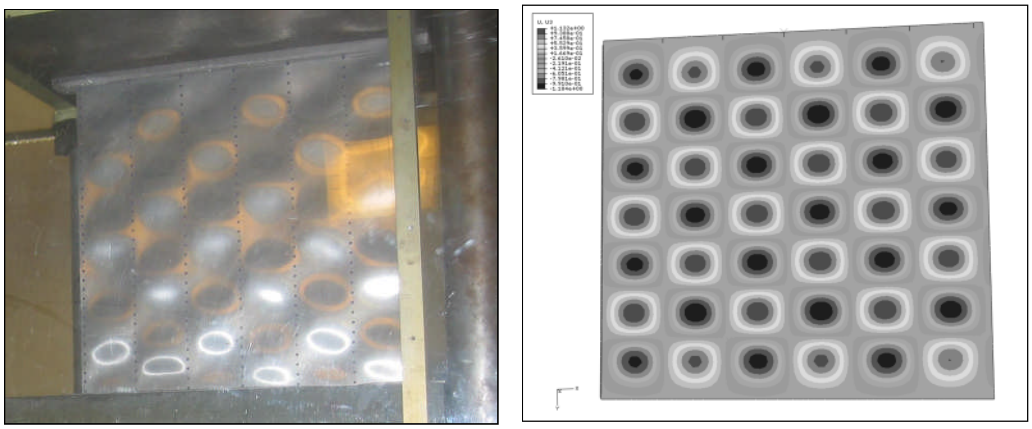

Figure 14: Local Buckling of Test Panel and Simulation (out-of plane displacement)

Fig. 14 compares the out-of-plane displacement of the test with the FEM solution during local buckling. Local buckling starts at about 23 kN in the simulation. This is close to the value from the design calculation. Test and simulation shape both have 3.5 wavelengths axially and look very similar.

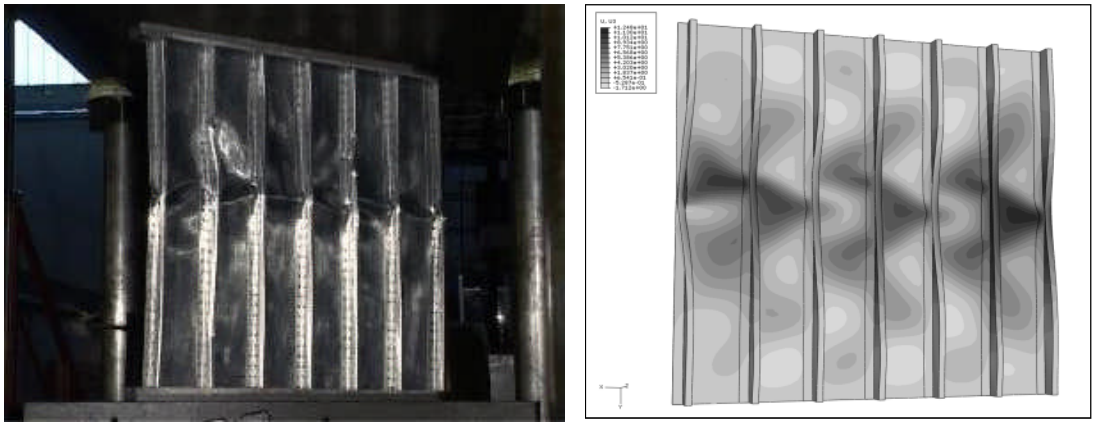

Figure 15: Collapse of Test Panel and Simulation (out-of plane displacement)

Fig. 15 compares the real and the calculated failure shape. The predicted torsional buckling is visible at the outer stiffeners, followed by flexural buckling.

5.9 Overall Error Assessment

Error Source	Analysis outcome	[%]
Material model	The model uses an appropriate elasto-plastic material model, but leaves an idealisation error.	1
Applying load / displacement	Application of displacement instead of load does not change the solution process.	-
Contact between panel and stiffener	A suitable rivet and contact model was found, but some uncertainty is left.	1
Sensitivity to boundary conditions	The Cerrobend modelling was improved. Panel end rotations cause an idealisation error.	3
Shape of the stiffeners	The final model includes curved shapes but leaves an idealisation error.	1
Geometrical imperfection	Local imperfections are incorporated in the model.	-
Scattering in material parameters	This error source was analysed using published material parameter variances.	1
Accordance with predicted failure modes	The solution shows correct behaviour and fails in accordance with the predicted mode (torsional buckling).	-

Table 11: Overall Error Assessment

Table 11 summarises the idealisation error analysis. “[%]” lists the determined idealisation errors present in the final model. In practice the error sources are not independent, but the interaction of the different error sources is specific to a problem and impractical to quantify. Following the idealisation error control process has allowed us to identify and quantify the errors introduced during this process. It is also

possible to use the results from the error assessment to identify a conservative model with the lowest failure load.

5.10 Final Model

The final model incorporated all improvements, as listed in Table 11. The model includes the curved stiffener shape with “3 elements per curve” and contains local imperfections of the measured magnitude. The analysis is displacement controlled and uses 379000 S4R shell elements. Increasing the number of elements is the consequence of a more complex model. It is important to place sufficient shell elements between two connector elements to model inter-rivet deformations. The maximum step size was set to 1% of the total applied displacement.

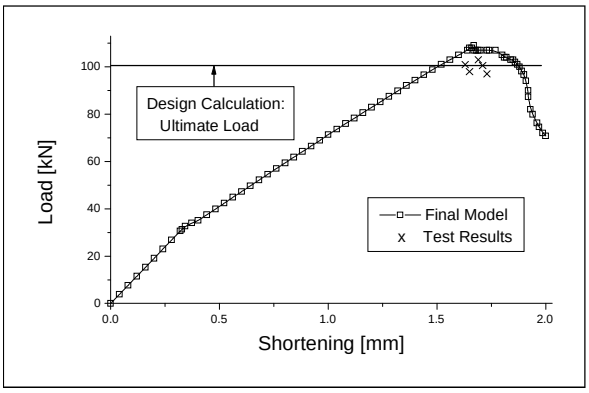

Figure 16: Final Model, Design Calculation and Test Data

Model	Collapse Load [kN]
Final model	108.60
Design calculation	100.83
Tests	97.00 .. 103.00

Table 12: Collapse Load of the Final Model, Design Calculation and Tests

The final model predicts a failure load of 108.60 kN, see Fig. 16 and Table 12. In tests ultimate strengths between 97 and 103 kN were measured. The design calculation is in accordance with the test results, but the FEM model overestimates the average measured test collapse load by 8%.

6. Conclusions

Using the SAFESA methodology for the investigated non-linear analysis leads to a better understanding of the FE idealisation process, and displays concrete error estimates. The investigated panel is very thin (skin and stringer thickness are both 0.9 mm), which leads to strong geometrical non-linearity. The study revealed that the main idealisation error sources are the stiffener shape, boundary conditions, material model and contact modelling. Geometrical imperfections did not show a large impact. The final FE model overestimates the mean test failure load by 8%.

Acknowledgements

The work presented in this paper was financially supported by the MUSCA Project "Non-linear static multiscale analysis of large aero-structures", partially funded by the European Union under the Sixth Framework Programme (Project Reference 516115). The authors would like to thank Prof. Dr. Alan Morris, Prof. Dr. Alan Rothwell, Prof. Dr. Jens Lang, Dr. Adrian Murphy and Dr. Matthias Heitmann for their helpful comments and the reviewers for their valuable feedback.

References

[1] Heitmann M, Horst P, Fitzsimmons D. Effective stiffness of postbuckled stiffened metallic panels under combined compression and shear stress. J. Strain Analysis 2003;38(6):539-555.
[2] Lynch C, Murphy A, Price M, Gibson A. The computational analysis of fuselage stiffened panels loaded in compression. Thin-Walled Structures 2004;42:1445-1464.
[3] Murphy A, Price M, Gibson A, Armstrong C G. Efficient non-linear idealisations of aircraft fuselage panels in compression. Finite Elements in Analysis and Design 2004;40:1978-1993.
[4] Morris A J, Vignjevic R. Consistent finite structural analysis and error control. Comput. Methods Appl. Mech. Engrg. 1997;140:87-108.
[5] Vignjevic R, Morris A J, Belagundu A D. Towards high fidelity finite element analysis. Adv Engng Software 1998;29(7-9):655-665.
[6] Hetey L, Idealisation error control for aerospace virtual structural testing. PhD Thesis, Cranfield University, Cranfield, England, 2009.
[7] Anonymous. ABAQUS/Standard user's manual, ver. 6.10, Hibbitt, Karlsson and Sorensen, 2010.
[8] ESDU 72012. Information on the use of data items on the buckling of plates and compression panels manufactured from isotropic materials. ESDU, 1972.
[9] Ramberg W, Osgood W R. Description of stress-strain curves by three parameters. NACA tech. note 902, 1943.
[10] Stressing Data Sheets, AVT-AVD 9632, Cranfield College of Aeronautics, 1999.
[11] Collette M, Strength and reliability of aluminium stiffened panels. PhD Thesis, University of Newcastle, Newcastle upon Tyne, England, 2005.
[12] ESDU. Metallic material data handbook. DEF STAN 00-932, ESDU International Ltd, 1990.
[13] DoD. Military standardization handbook. Metallic materials and elements for aerospace vehicle structures, MIL-HDBK-5, USA, Department of Defence, 2001.
[14] Haugen E B. Probabilistic mechanical design. Wiley, 1980.